Identification of Oxidized Derivatives of Neuroketals†

Nathalie Bernoud-Hubac and L. Jackson Roberts, II*

Departments of Pharmacology and Medicine, Vanderbilt University, Nashville, Tennessee 37232-6602

Received February 27, 2002; Revised Manuscript Received August 4, 2002

ABSTRACT: Oxidative stress and protein aggregation have been implicated in the pathogenesis of neurodegenerative diseases. The formation of neuroprostanes, isoprostane-like compounds formed from oxidation of docosahexaenoic acid, which is uniquely enriched in the brain, is increased in Alzheimer's disease. We recently identified the formation of a new class of highly reactive γ-keto aldehydes, neuroketals, in vivo as products of the neuroprostane pathway. Neuroketals adduct to lysine residues of proteins with remarkable rapidity and induce cross-linking. Because neuroketals have either a 1,4-pentadiene or 1,4,7-octatriene side chain structure, we hypothesized that they could undergo further oxidation to form neuroketals with an additional hydroxyl group. Oxidation of docosahexaenoic acid in vitro yielded a series of compounds that were confirmed to be oxidized neuroketals by mass spectrometric analyses. Analysis of oxidized neuroketal adducts during oxidation of docosahexaenoic acid in the presence of lysine revealed the formation of oxidized Schiff base and hydroxylactam adducts. Oxidized hydroxylactam neuroketal-lysyl protein adducts, analyzed after digestion of proteins to individual amino acids, were not detected in nonoxidized rat brain synaptosomes but were readily detected following oxidation of synaptosomes. These studies indicate that neuroketals can undergo further oxidation, which in turn suggests that measurement of only unoxidized neuroketal adducts likely underestimates the amount of neuroketal adducts present in the brain in disorders of oxidant stress.

We previously described the formation of highly reactive γ-keto aldehydes, isoketals (IsoKs),[1] as products of the isoprostane pathway of free radical-induced peroxidation of arachidonic acid (AA) (*1*). The γ-keto aldehyde moiety of these molecules reacts with the ϵ-amine of lysine residues on proteins to form a Schiff base adduct and pyrrole-derived lactam and hydroxylactam adducts (*1*, *2*). It is of particular relevance that IsoKs are at least an order of magnitude more reactive than 4-hydroxynonenal, which is considered to be one of the most reactive products of lipid peroxidation (*1*). In addition, IsoKs exhibit a strong proclivity to induce protein−protein cross-links. More recently, we reported that reactive IsoK-like compounds (neuroketals, NKs) are formed as abundant products of the neuroprostane (NP) pathway of free radical-catalyzed peroxidation of docosahexaenoic acid (DHA) (*3*). NKs were also shown to rapidly adduct to lysine, forming lactam and Schiff base adducts.

Oxidative stress has been strongly implicated in the pathogenesis of Alzheimer's disease, and cross-linked protein aggregates are a feature of the disease (*4*−*9*). The underlying mechanism(s) responsible for protein aggregation and cross-linking in Alzheimer's disease is (are) not well understood. We have previously reported that the formation of products of the isoprostane pathway is increased in Alzheimer's disease and more recently that the formation of products of the neuroprostane pathway is increased to an even greater extent (*6*, *7*, *9*). Perhaps relevant in this regard was our observation that the amounts of NKs formed during co-oxidation of AA and DHA in vitro exceed that of IsoKs (*3*). This, therefore, makes NKs an attractive candidate for being involved in protein aggregation and cross-linking in Alzheimer's diseases.

Eight regioisomers of NKs are formed, each comprised of eight racemic diastereomers. Of these eight regioisomers, four have a 1,4-pentadiene structure and four have a 1,4,7-octatriene structure on one of the side chains. Because these pentadiene and octatriene structures would potentially be susceptible to further oxidation as shown in Figure 1, we sought to determine the extent to which this occurs. Shown in Figure 1 is the process by which a single NK regioisomer with a 1,4-pentadiene side chain structure can undergo further oxidation by insertion of a third atom of oxygen. The addition of the third atom of oxygen could occur before rearrangement of the bicyclic endoperoxide to the γ-keto aldehyde as shown in the figure, after rearrangement of the bicyclic endoperoxide, or even after adduction of the NK to lysine residues on proteins.

Our interest in determining the extent to which NKs undergo further oxidation relates to the measurement of NK protein adducts in vivo. If a significant fraction of NKs undergo further oxidation in vivo, measurement of only unoxidized NK adducts would underestimate the amount of NKs that participate in the formation of protein adducts in the brain in disorders of oxidative stress, e.g., neurodegenerative diseases.

† This work was supported by National Institutes of Health Grants GM42056, GM15431, CA68485, and DK26657.

* To whom correspondence should be addressed. Tel: 615-343-1816. Fax: 615-343-9446. E-mail: jack.roberts@mcmail.vanderbilt.edu.

[1] Abbreviations: AA, arachidonic acid; DHA, docosahexaenoic acid; CID, collision-induced dissociation; ESI, electrospray ionization; GC, gas chromatography; HPLC, high-pressure liquid chromatography; IsoK, isoketal; MS, mass spectrometry; MS/MS, tandem mass spectrometry; NICI, negative ion chemical ionization; NK, neuroketal; SRM, selected ion monitoring; TLC, thin-layer chromatography.

10.1021/bi0257383 CCC: $22.00
Published on Web 08/30/2002

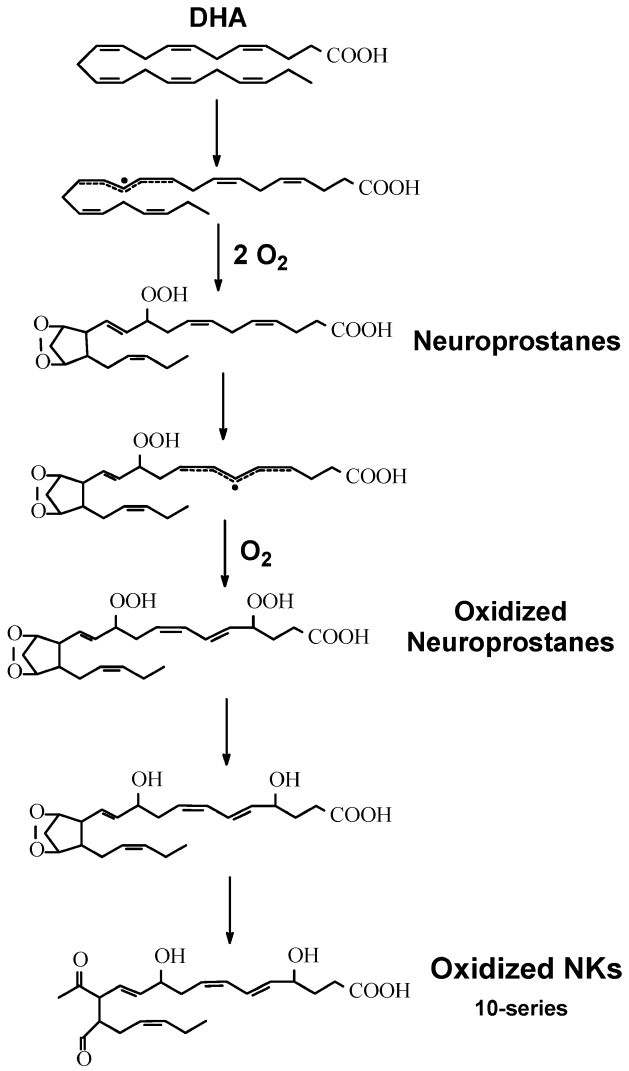

FIGURE 1: Pathway for the formation of oxidized NKs by nonenzymatic peroxidation of DHA. A DHA radical is initially generated which, following addition of molecular oxygen, results in the formation of a bicyclic endoperoxide intermediate. Following insertion of a third molecule of oxygen, the peroxy groups are reduced, and the bicyclic endoperoxide intermediate rearranges to form oxidized NKs.

MATERIALS AND METHODS

Materials. Ammonium acetate, *N*,*N*-dimethylformamide, trolox, undecane, and triphenylphosphine were purchased from Aldrich (Milwaukee, WI). Docosahexaenoic acid was from Nu-Chek-Prep, Inc. (Elysian, MN). L-[4,5-^{3}H]Lysine was from PerkinElmer Life Sciences. [$^{13}C_6$]-L-Lysine and [$^2H_3$]methoxyamine hydrochloride were from Cambridge Isotope Laboratories, Inc. (Andover, MA). Butylated hydroxytoluene, methoxyamine hydrochloride, pentafluorobenzyl bromide, and sodium borohydride were from Sigma (St. Louis, MO). *N*,*O*-Bis(trimethylsilyl)trifluoroacetamide was from Regis Chemical (Morton Grove, IL). [$^2H_9$]-*N*,*O*-Bis(trimethylsilyl)trifluoroacetamide was from CDP isotopes (Pointe-Claire, PQ). Porcine aminopeptidase M (60 units/mL) and Pronase were from Calbiochem (La Jolla, CA). C18 Sep Pak cartridges and Oasis cartridges were from Waters Associates (Milford, MA). Male Sprague-Dawley rats were from Harlan Sprague-Dawley, Inc. (Indianapolis, IN).

Oxidation of DHA. DHA (5 mg) was oxidized in vitro using a mixture of iron (1 mM), ADP (200 mM), and ascorbate (100 mM) in 5 mL of 1 × phosphate-buffered saline at room temperature for 2 h as described (*10*).

Gas Chromatography (GC)/Negative Ion Chemical Ionization (NICI)/Mass Spectrometry (MS) Analysis of Oxidized NKs. The technique used to purify and analyze oxidized NKs is similar to that described for NKs (*3*). Following oxidation of DHA, oxidized NKs were converted to *O*-methyloxime derivatives, extracted using a C18 Sep Pak cartridge, converted to a pentafluorobenzyl ester derivative, and purified by thin-layer chromatography (TLC). NKs migrate in the region on the TLC plate that extends between 0.5 cm above to 1.5 cm above where the *O*-methyloxime pentafluorobenzyl ester derivative of [$^2H_4$]PGE_2 migrates. If oxidized NKs containing an additional hydroxyl group are formed, they would be expected to migrate in a more polar region of the TLC plate. Therefore, we scraped the region for oxidized NKs that extended from 0.5 cm below to 0.5 cm above the PGE_2 standard. This area was determined to contain oxidized NKs by analyzing sequential small cuts of the TLC plate for compounds. The compounds were then converted to a trimethylsilyl ether derivative and analyzed by GC/NICI/MS using selected ion monitoring of the M − $^{\bullet}CH_2C_6F_5$ ions at *m*/*z* 535 for oxidized NKs and *m*/*z* 528 for the [$^2H_4$]PGE_2 internal standard. Catalytic hydrogenation was performed as described (*11*).

Liquid Chromatography (LC)/Electrospray Ionization (ESI)/MS/MS Analysis of NK-Lysyl Adducts. The purification and analysis of oxidized NK-lysyl adducts followed similar procedures used for purification and analysis of NK-lysyl adducts (*3*). Briefly, DHA (10 mg) was incubated with lysine (10 mg) and oxidized as described above. One-tenth volume of 1 M sodium borohydride in dimethylformamide was added, and the mixture was incubated for 30 min at 4 °C to reduce and stabilize oxidized Schiff base adducts. After extraction with an Oasis cartridge, the adducts were analyzed by LC/ESI/MS/MS operating in the positive ion mode using a 2.1 × 15 mm XDB C8 column (MacMod Analytical) with a flow rate of 0.2 mL/min as described previously (*1*, *3*). The solvent system employed was a linear gradient of 10−90% acetonitrile in 5 mM ammonium acetate/0.1% acetic acid. The sheath gas pressure was held at 70 psi and the auxiliary gas pressure at 10 psi. The tube lens was 80 V, and the voltage on the capillary was 20 V. Molecular ions of putative oxidized NK-lysyl adducts were subjected to collision-induced dissociation (CID) from −20 to −40 eV with 2.6 mTorr collision gas, scanning daughter ions between 50 and 550.

Analysis of Oxidized NK-Lysyl Adducts in Synaptosomes. Synaptosomes were prepared from adult male Sprague-Dawley rats by the method of Janowsky et al. (*12*). An iron/ADP/ascorbate mixture (1 mM/200 mM/100 mM) was added to the synaptosomal preparation to initiate lipid peroxidation. Incubations were carried out at 37 °C for 6 h. Placing the samples at −80 °C terminated the reactions. Following base hydrolysis, proteins were precipitated, washed, and subjected to complete enzymatic digestion to individual amino acids as previously described (*3*). Oxidized NK-lysyl adducts were then extracted by an Oasis cartridge and HPLC on a 4.6 × 250 mm Macrosphere 300 C18 column (MacMod Analytical; Chadds Ford, PA) as described (*3*). One minute HPLC

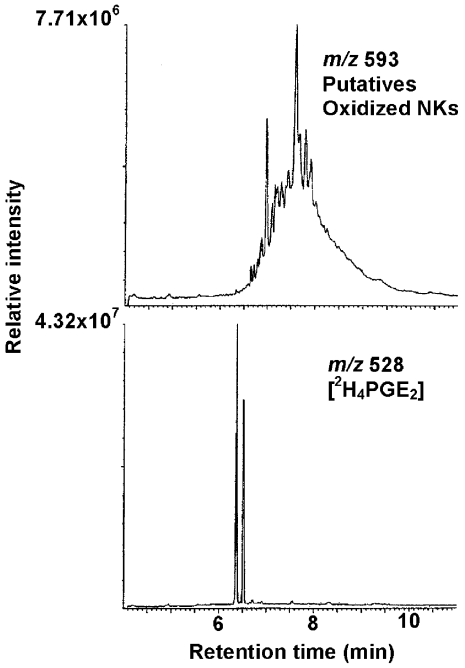

FIGURE 2: Selected ion current chromatograms from the analysis of the formation of oxidized NKs generated during iron/ADP/ascorbate-induced oxidation of DHA in vitro. The series of peaks in the *m*/*z* 593 chromatogram represent putative oxidized NKs. The peaks in the *m*/*z* 528 chromatogram represent the *syn*- and *anti*-*O*-methyloxime isomers of the $[^2H_4]PGE_2$ internal standard.

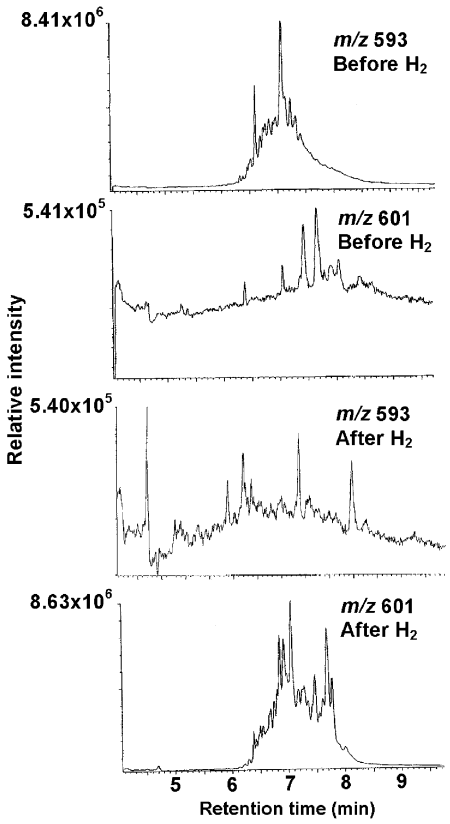

FIGURE 3: Analysis of putative oxidized NKs formed during oxidation of DHA prior to and after catalytic hydrogenation. Intense peaks are present in the *m*/*z* 593 ion current chromatogram representing oxidized NKs, and no peaks were detected 8 Da above *m*/*z* 593 at *m*/*z* 601 prior to hydrogenation. Following catalytic hydrogenation the *m*/*z* 593 peaks shifted upward 8 Da, indicating that the *m*/*z* 593 compounds have four double bonds.

fractions containing radioactivity from oxidized NK-lysyl adduct internal standards were combined, reextracted with Oasis cartridges, and analyzed by LC/ESI/MS/MS as described above. Standards were synthesized as follow. DHA (20 mg) was incubated with 2 mg of $[^{13}C_6]$lysine and $[^3H]$lysine (50×10^6 cpm) in 1 × phosphate-buffered saline. The mixture was extracted using an Oasis cartridge and then by HPLC as described above. One minute fractions were collected, and aliquots containing radioactivity were analyzed and quantified by LC/ESI/MS/MS.

RESULTS

Formation of Oxidized NKs in Vitro. We initially explored whether oxidized NKs with an additional hydroxyl group are formed in vitro during oxidation of DHA with iron/ADP/ascorbate. A representative selected ion current chromatogram obtained from this analysis is shown in Figure 2. The two chromatographic peaks in the lower *m*/*z* 528 chromatogram represent the *syn*- and *anti*-*O*-methyloxime isomers of the internal standard $[^2H_4]PGE_2$. The *m*/*z* 593 ion would be the expected M − $^{\bullet}CH_2C_6F_5$ ion for oxidized NKs. Shown at the top is the *m*/*z* 593 ion current chromatogram in which multiple peaks are present at a slightly longer retention time than that of PGE_2, as would be expected since NKs contain an additional two carbon atoms.

Additional studies were then undertaken to confirm the identity of the compounds in the *m*/*z* 593 ion current chromatogram as oxidized NKs. First, no *m*/*z* 592 peaks were present, indicating that the *m*/*z* 593 peaks are not natural isotopes of compounds generating an ion less than *m*/*z* 593. When analyzed as a $[^3H_9]$trimethylsilyl ether derivative and $[^2H_3]$-*O*-methyloxime derivative, all of the original *m*/*z* 593 chromatographic peaks disappeared, and an identical pattern of new peaks appeared 18 and 6 Da higher, respectively (not shown). This indicated that all of the compounds had two hydroxyl groups and two carbonyl groups. When oxidized NKs were analyzed prior to catalytic hydrogenation, there were no peaks present at *m*/*z* 601. However, following catalytic hydrogenation, there was a disappearance of the *m*/*z* 593 chromatographic peaks and the appearance of new intense peaks 8 Da above *m*/*z* 593 at *m*/*z* 601 (Figure 3), indicating the presence of four double bonds.

Identification of Oxidized NK-Lysyl Adducts. IsoKs and NKs initially react with the ϵ-amine of lysine residues to form a reversible Schiff base adduct (*2*, *3*) which then irreversibly cyclizes to a pyrrole. The pyrrole then undergoes autoxidation to form stable lactam adducts (*1*, *3*) and hydroxylactam adducts (*1*). We then analyzed for the formation of oxidized NK lysine adducts during oxidation of DHA in the presence of lysine by iron/ADP/ascorbate for 4 h. Then, following reduction by sodium borohydride, the reaction mixture was analyzed by LC/ESI/MS in the positive ion mode. Figure 4 shows selected ion current chromatograms of *m*/*z* 507, *m*/*z* 519, and *m*/*z* 535 obtained from these analyses. The *m*/*z* 507 ion is of lower intensity compared to the *m*/*z* 519 and 535 ions. The *m*/*z* 507 ion is the predicted $[MH]^+$ ion for the oxidized NK-lysyl reduced Schiff base adduct that has lost one molecule of water. This is consistent with our previous work with IsoKs and NKs showing that dehydration occurs during reduction of the imine and carbonyl groups with sodium borohydride (*2*, *3*). The

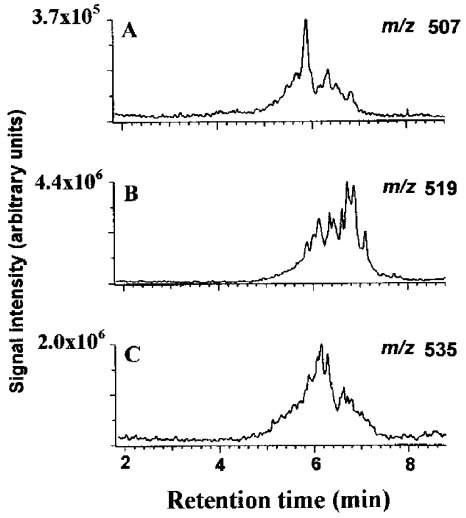

FIGURE 4: DHA was oxidized with iron/ADP/ascorbate in the presence of lysine. Oxidized NK adducts were then analyzed by LC/ESI/MS. Selected ion current chromatograms of the putative oxidized NK-lysyl reduced Schiff base adducts (A), hydroxylactam and oxidized NK-lysyl lactam adducts (B), and oxidized NK-lysyl hydroxylactam adducts (C) are shown. See Figure 6 for the structures of these adducts.

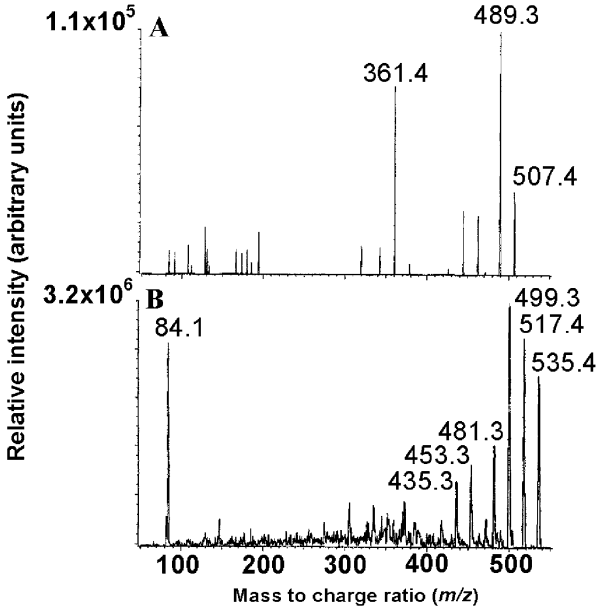

FIGURE 5: Collision-induced dissociation spectrum of the MH^+ ion *m/z* 507 of oxidized NK-lysyl reduced Schiff base adducts (A) and the MH^+ ion *m/z* 535 of oxidized NK-lysyl hydroxylactam adducts (B). Oxidized NK-lysyl adducts formed during oxidation of DHA in the presence of lysine were subjected to CID at −28 eV. Daughter ions were scanned between *m/z* 50 and *m/z* 550. The proposed structures of individual ions are shown in Figure 6.

predicted $[MH]^+$ ion for the oxidized NK-lysyl hydroxylactam adducts is *m/z* 535. The *m/z* 519 peaks are consistent with the formation of oxidized NK-lysyl lactam adducts. However, the *m/z* 519 is also the expected molecular ion $[MH]^+$ of the NK-lysyl hydroxylactam adducts. Therefore, it is likely that the *m/z* 519 peaks represent a mixture of NK-lysyl hydroxylactam and oxidized NK-lysyl lactam adducts.

Further structural characterization of the *m/z* 507 and *m/z* 535 peaks was then undertaken to confirm their identity as oxidized NK Schiff base and hydroxylactam adducts by analysis of the daughter ions produced upon CID (Figure 5). Prominent daughter ions present in the CID spectrum of putative oxidized NK Schiff base adducts were *m/z* 489 and *m/z* 361 (Figure 5A). Prominent daughter ions present in the CID spectrum of the putative oxidized NK hydroxylactam adducts include *m/z* 517, *m/z* 499, *m/z* 481, *m/z* 453, *m/z* 435, and *m/z* 84 (Figure 5B). On the basis of analogous daughter ions obtained upon CID of IsoK- and NK-lysyl adducts (*1*, *3*), fragment ions can be interpreted as shown in Figure 6. LC/ESI/MS/MS analysis of the ions at *m/z* 519 did not provide unique fragmentation ions that allowed a distinction between hydroxylactam and oxidized lactam adducts (not shown).

Formation of Oxidized NK Hydroxylactam Adducts in Oxidized Synaptosomes. We then undertook experiments to determine whether oxidized NK adducts could be detected in a biological system using rat brain synaptosomes as a model. Lactam, hydroxylactam/oxidized lactam, and oxidized hydroxylactam NK adducts were isolated following enzymatic digestion of proteins to individual amino acids and quantified by LC/ESI/MS/MS using selected reaction monitoring (SRM) of the transition of the $[MH]^+$ ions to the specific daughter ion *m/z* 84. Figure 7A represents the SRM of the $[MH]^+$ ion *m/z* 541 for the oxidized NK $[^{13}C_6]$lysyl hydroxylactam adduct internal standard to *m/z* 89. In panels B and C of Figure 7 are shown the *m/z* 535 to *m/z* 84 ion current chromatograms for oxidized NK hydroxylactam adducts in the synaptosomes. Oxidized hydroxylactam adducts were not detected in nonoxidized synaptosomes (Figure 7B). However, following oxidation of synaptosomes for 6 h with iron/ADP/ascorbate, intense peaks were present, indicating the presence of oxidized NK hydroxylactam adducts at a level of 0.59 ng/mg of protein (Figure 7C). The relative amounts of lactam, the mixture of oxidized lactam and hydroxylactam (which as mentioned cannot be distinguished), and oxidized hydroxylactam adducts formed over time are summarized in Table 1. The levels of the different adduct species all increased dramatically during the first 2 h of oxidation of the synaptosomes but only increased slightly after 2 h. Although we did not determine this, this might be explained by depletion of a major amount of unoxidized DHA during the first 2 h of the incubation. The major conclusion that can be reached from these data is that the amount of oxidized hydroxylactam plus some fraction of the mixture of oxidized lactam and hydroxylactam representing oxidized lactam is not an inconsequential fraction of the total amount of adducts formed.

DISCUSSION

We report the finding that oxidized NKs are formed during oxidation of DHA in vitro and in a model system of oxidant injury in vivo (oxidized synaptosomes). Our interest in understanding the spectrum of the fate of NKs stems from the hypothesis that the formation of NKs may be important in the pathogenesis of neurodegenerative diseases. This is an attractive hypothesis in light of the fact that the γ-keto aldehyde moiety of NKs and IsoKs confers unique chemical and biological properties and because we have previously reported that products of the neuroprostane pathway are significantly increased both in cerebrospinal fluid and in brain from patients with Alzheimer's disease (*6*, *9*). These γ-keto aldehydes form covalent adducts with proteins at a rate that

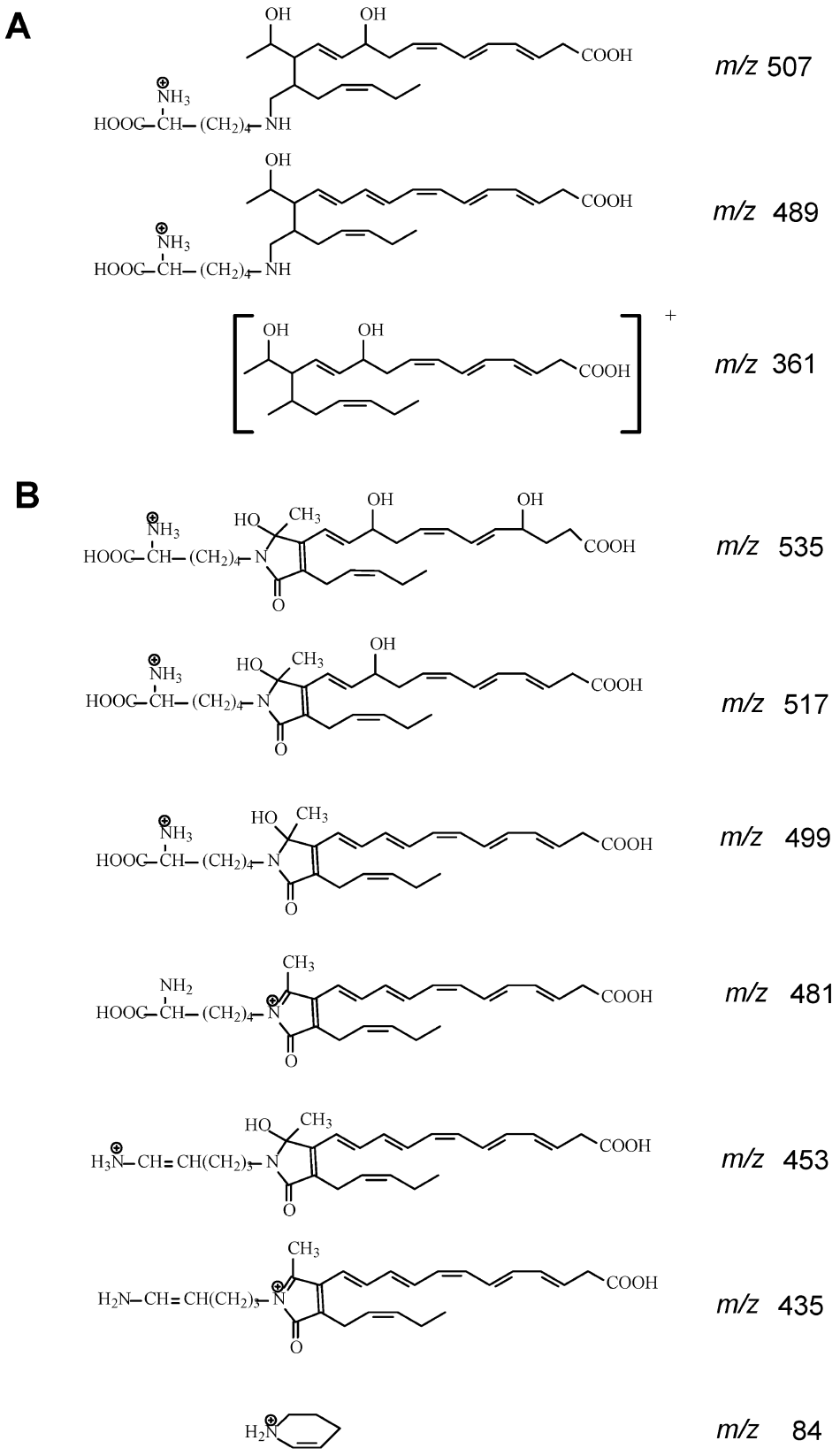

FIGURE 6: Interpretation of the fragmentation ions in the CID spectrum of the oxidized NK-lysyl reduced Schiff base adducts (A) and oxidized NK-lysyl hydroxylactam adducts (B).

exceeds that of 4-hydroxynonenal by more than a order of magnitude, and they also exhibit a unique proclivity to cross-link proteins. The latter property of NKs may be important in the context that aggregated cross-linked proteins are a feature of Alzheimer's disease and its cause remains poorly understood. Moreover, we recently found that IsoK-adducted proteins are poorly degraded by the proteasome and they also inhibit the proteasome from degrading normal substrates (*13*), both of which can lead to protein accumulation and aggregation. Moreover, inhibition of proteasome function in

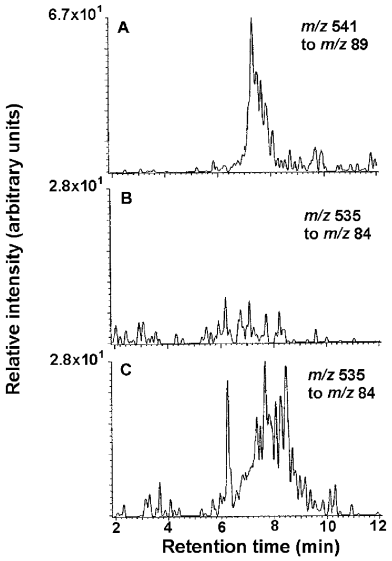

FIGURE 7: LC/ESI/MS/MS analysis of oxidized NK-lysyl hydroxylactam adducts from nonoxidized rat brain synaptosomes (B) and oxidized synaptosomes (C). Analysis of lysine adducts was performed following complete enzymatic digestion of synaptosomal proteins to individual amino acids. The internal standards consisting of $^{13}C_6$, ^{3}H oxidized NK-lysyl hydroxylactam adducts, formed by oxidation of DHA in the presence of [$^{13}C_6$]lysine and [^{3}H]lysine, were then added. SRM of the following transitions was performed: *m*/*z* 541 to *m*/*z* 89 (internal standard, A) and *m*/*z* 535 to *m*/*z* 84 (oxidized hydroxylactam adducts from nonoxidized synaptosomes, B, and from oxidized synaptosomes, C).

Table 1: Levels of NK-Lysyl Lactam Adducts, NK-Lysyl Oxidized Hydroxylactam Adducts, and NK-Lysyl Oxidized Lactam + Hydroxylactam Adducts in Nonoxidized Synaptosomes and in Synaptosomes Oxidized for 2, 4, and 6 h[a]

	0 h	2 h	4 h	6 h
lactam	0.09[b]	1.18	1.04	1.56
oxidized OH-lactam	0	0.34	0.42	0.59
oxidized lactam + OH-lactam	0.09	0.74	0.67	1.06

[a] Synaptosomes were subjected to oxidation by iron/ADP/ascorbate, delipidated, and subjected to complete enzymatic hydrolysis to individual amino acids. [b] Levels are expressed as ng/mg of protein.

neuronal cells leads to apoptosis (*14*, *15*). IsoKs also potently induced cell death in P19 neuroglial cells at submicromolar concentrations. These effects of IsoK adducted proteins and IsoKs on proteasome function and cytotoxicity occurred at concentrations that were orders of magnitude lower than what has been observed for 4-hydroxynonal adducted proteins and 4-hydroxynonenal. Although the effect of NK adducted proteins on proteasome function and the effect of NKs on cytotoxicity have not be investigated due to the unavailability of a synthetic NK, there would be no reason to expect that the effect of NKs would be different than that of the IsoKs.

In an attempt to explore the role of NKs in neurodegenerative diseases, it is key to determine if they are present in brain in amounts sufficient to induce pathobiology. In this context, it is important to determine all forms in which they can occur in vivo. Thus we considered that NKs may undergo further oxidation owing to the presence of 1,4-pentadiene and 1,4,7-octatriene structures on the side chains. We found that oxidized hydroxylactams were readily detectable during oxidation of DHA and, more importantly, during oxidation of a biological system, brain synaptosomes. We could not distinguish between hydroxylactam and oxidized lactams since they have the same mass, but since oxidized hydroxylactams were present, oxidized lactams are also likely present. These findings suggest that the best approach to assess levels of NK adducts in brain is to measure the sum of lactams, oxidized lactams/hydroxylactams, and oxidized hydroxylactams. It follows, therefore, that measurement of only nonoxidized NK adducts would underestimate the amount of NK adducts in brain. It may be worthy of mention that the conditions used in these studies may not closely mimic those in vivo. As mentioned, we found that IsoK adducted proteins are degraded very poorly by the proteasome. Accordingly, the NK adducted proteins may have a very prolonged half-life in the brain. This would favor conditions that would allow further oxidation of NK protein adducts in vivo, in which case the amount of more oxidized NKs may be more abundant in vivo than detected during the short incubations used in the experiments described in this current work.

REFERENCES

1. Brame, C. J., Salomon, R. G., Morrow, J. D., and Roberts, L. J. (1999) *J. Biol. Chem. 274*, 13139−13146.
2. Boutaud, O., Brame, C. J., Salomon, R. G., Roberts, L. J., and Oates, J. A. (1999) *Biochemistry 38*, 9389−9396.
3. Bernoud-Hubac, N., Davies, S. S., Boutaud, O., Montine, T. J., and Roberts, L. J., II (2001) *J. Biol. Chem. 276*, 30964−30970.
4. Masters, C. L., Simms, G., Weinman, N. A., Multhaup, G., McDonald, B. L., and Beyreuther, K. (1985) *Proc. Natl. Acad. Sci. U.S.A. 82*, 4245−4249.
5. Glenner, G. G. (1988) *Cell 52*, 307−308.
6. Roberts, L. J., II, Montine, T. J., Markesbery, W. R., Tapper, A. R., Hardy, P., Chemtob, S., Dettbarn, W. D., and Morrow, J. D. (1998) *J. Biol. Chem. 273*, 13605−13612.
7. Montine, T. J., Markesbery, W. R., Morrow, J. D., and Roberts, L. J. (1998) *Ann. Neurol. 44*, 410−413.
8. Markesbery, W. R. (1999) *Arch. Neurol. 56*, 1449−1452.
9. Reich, E. E., Markesbery, W. R., Roberts, L. J., II, Swift, L. L., Morrow, J. D., and Montine, T. J. (2001) *Am. J. Pathol. 158*, 293−297.
10. Longmire, A. J., Swift, L. L., Roberts, L. J., II, Awad, J. A., Burke, R. F., and Morrow, J. D. (1994) *Biochem. Pharmacol. 47*, 1173−1177.
11. Morrow, J. D., Harris, T. M., and Roberts, L. J. (1990) *Anal. Biochem. 184*, 1−10.
12. Janowsky, A., Neve, K., and Eshleman, A. J. (1998) *Current protocols in neurosciences*, John Wiley and Sons, New York.
13. Davies, S. S., Armanath, V., Montine, K. S., Bernoud-Hubac, N., Boutaud, O., Montine, T. J., and Roberts, L. J., II (2002) *FASEB J., 10.*1096/fj.01-0696fje.
14. Lopes, U. G., Erhardt, P., Yao, R., and Cooper, G. M. (1997) *J. Biol. Chem. 272*, 12893−12896.
15. Taglialatela, G., Robinson, R., and Perez-Polo, J. R. (1997) *J. Neurosci. Res. 47*, 155−162.

BI0257383